Analytica Chimica Acta 1154 (2021) 338325

Contents lists available at ScienceDirect

Analytica Chimica Acta

journal homepage: www.elsevier.com/locate/aca

Gas chromatography-mass spectrometry based ^{18}O stable isotope labeling of Krebs cycle intermediates

Cemil Can Eylem [a], İpek Baysal [b], Acelya Erikci [c], Samiye Yabanoglu-Ciftci [d], Song Zhang [e], Sedef Kır [a], Andre Terzic [e], Petras Dzeja [e], Emirhan Nemutlu [a, *]

[a] Hacettepe University, Faculty of Pharmacy, Department of Analytical Chemistry, Ankara, Turkey
[b] Hacettepe University, Hacettepe University, Vocational School of Health Services, Ankara, Turkey
[c] Lokman Hekim University, Faculty of Pharmacy, Department of Biochemistry, Ankara, Turkey
[d] Hacettepe University, Faculty of Pharmacy, Department of Biochemistry, Ankara, Turkey
[e] Department of Cardiovascular Medicine, Mayo Clinic, Rochester, MN, USA

HIGHLIGHTS

- ^{18}O isotope labeling can be used for flux analysis of Krebs Cycle metabolites.
- ^{18}O isotope labeling can be used for the labeling of phosphate-containing and non-phosphate metabolites.
- For the first time, ^{18}O stable isotopes were used to track non-phosphate containing metabolites.
- ^{18}O isotope labeling allows to track more pathways than ^{13}C or ^{15}N isotope labeling anologs.
- ^{18}O isotope labeling results revealed the Warburg effect on Caco-2 cell lines.

GRAPHICAL ABSTRACT

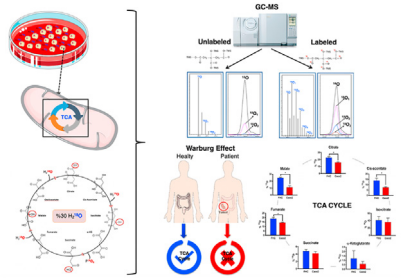

ARTICLE INFO

Article history:
Received 10 December 2020
Received in revised form
7 February 2021
Accepted 11 February 2021
Available online 16 February 2021

Keywords:
^{18}O stable isotope labeling
Gas chromatography-mass spectrometry
Krebs cycle
Citric acid cycle

ABSTRACT

New technologies permit determining metabolomic profiles of human diseases by fingerprinting metabolites levels. However, to fully understand metabolomic phenotypes, metabolite levels and turnover rates are necessary to know. Krebs cycle is the major hub of energy metabolism and cell signaling. Traditionally, ^{13}C stable isotope labeled substrates were used to track the carbon turnover rates in Krebs cycle metabolites. In this study, for the first time we introduce $H_2[^{18}O]$ based stable isotope marker that permit tracking oxygen exchange rates in separate segments of Krebs cycle. The chromatographic and non-chromatographic parameters were systematically tested on the effect of labeling ratio of Krebs cycle mediators to increase selectivity and sensitivity of the method. We have developed a rapid, precise, and robust GC-MS method for determining the percentage of ^{18}O incorporation to Krebs cycle metabolites. The developed method was applied to track the cancer-induced shift in the Krebs cycle dynamics of Caco-2 cells as compared to the control FHC cells revealing Warburg effects in Caco-2 cells. We demonstrate that unique information could be obtained using this newly developed ^{18}O-labeling

Abbreviations: (KEGG) database, Kyoto Encyclopedia of Genes and Genomes; (Caco-2), Human colon adenocarcinoma cell lines; (FHC), Human fetal colon cell lines; (DMEM), Dulbecco's Modified Eagle Medium; (HEPES), 4-(2-hydroxyethyl)-1-piperazine ethanesulfonic acid; (DMEM-F12), Dulbecco's Modified Eagle Medium/Nutrient Mix F-12; (MSTFA), N-methyl- N-trimethylsilyl trifluoroacetamide; (TMCS), 1% trimethylchlorosilane; (GC-MS), Gas Chromatography-Mass Spectrometry.

* Corresponding author. Hacettepe University, Pharmacy Faculty Department of Analytical Chemistry, 06230, Sıhhiye, Ankara, Turkey.
E-mail addresses: cemilcaneylem@gmail.com (C.C. Eylem), ipekbysl@gmail.com (İ. Baysal), acelya.erikci@lokmanhekim.edu.tr (A. Erikci), samiye@hacettepe.edu.tr (S. Yabanoglu-Ciftci), zhang.song@mayo.edu (S. Zhang), sekir@hacettepe.edu.tr (S. Kır), terzic.andre@mayo.edu (A. Terzic), dzeja.petras@mayo.edu (P. Dzeja), enemutlu@hacettepe.edu.tr (E. Nemutlu).

https://doi.org/10.1016/j.aca.2021.338325

Warburg effect
Colon adenocarcinoma

analytical technology by following the oxygen exchange rates of Krebs cycle metabolites. Thus, ^{18}O-labeling of Krebs cycle metabolites expands the arsenal of techniques for monitoring the dynamics of cellular metabolism. Moreover, the developed method will allow to apply the ^{18}O-labeling technique to numerous other metabolic pathways where oxygen exchange with water takes place.

1. Introduction

The identification of metabolic pathways that are affected in diseases allows individualization of early diagnosis and treatment based on results of molecular differences [1]. Characterization of metabolic phenotypes requires determination of not only metabolite levels but also turnover rates. In particular, many metabolites are present at low concentrations and may have high flux or turnover rates [2]. On the other hand, significant changes in metabolic flux may occur without significant changes in metabolic concentration. Therefore, metabolomic profiling and flux measurements are crucial for a complete understanding of metabolic dynamics [3–6]. These types of analyses, which are based on the calculation of the metabolite levels as well as the turnover rates, are called fluxomics [7,8].

In general, fluxomic analysis can be performed using stable isotope (^{13}C, ^{15}N and ^{18}O) tracer-based metabolomic technologies allowing simultaneous determinations of metabolite levels and their turnover rates with subsequent evaluation of metabolic network dynamics [8–10]. Different stable isotopes are used for different pathways in fluxomic analyzes [8,11,12]. ^{13}C isotope and ^{15}N are widely used to monitor carbon backbone and nitrogen backbone, respectively [13,14]. On the other hand, ^{18}O, a natural and stable isotope, allows monitoring phosphotransfer networks and phosphoryl metabolic dynamics, which are responsible for energy and signal transduction [15–18]. Furthermore, the labeling period with ^{18}O is very short, unlike ^{13}C and ^{15}N isotope labeling experiments. Another advantage of $H_2[^{18}O]$ based labeling is its high equilibration rate in cellular water compared to ^{13}C and ^{15}N labeling experiments. Because water has a very high diffusion coefficient (2.3 μm^2/ms). On the other hand, ^{13}C labeled glucose (100–400 nmol/10^6 cells/h), and glutamine (30–100 nmol/10^6 cells/h) needs higher time for cellular uptake [19]. This allows water-based isotope tracer studies for more homogenous labeling in cell components and lowers labeling time [8].

The amalgamation of ^{18}O with metabolites happens only under enzymatic conditions, and the integration percentage of ^{18}O is directly proportional to the activity of the enzyme [12]. Thus, the turnover rate and the number of turnovers of the respective enzyme can be calculated by using ^{18}O labeling ratio [8].

^{18}O isotopes are suitable to follow cellular phosphorus turnover and metabolic dynamics of phosphoryl containing metabolites [2,8,20,21]. So far, analytical methods based on ^{18}O labeling are available only for a limited number of phosphometabolites (glucose-1-phosphate, glucose-6-phosphate, glycerol-3-phosphate, inorganic phosphate, creatininphosphate, AMP, ADP, ATP, GMP, GDP, and GTP). These ^{18}O labeled metabolites allow the tracking of various energy metabolic pathways such as ATP synthesis and use, adenylate kinase, creatine kinase, and glycolytic phosphotransfer pathways, energy transfer and glycogen turnover [22–24]. Although $H_2[^{18}O]$ is used as the label carrier, and there are approximately 3000 enzymatic reactions involving water according to the Kyoto Encyclopedia of Genes and Genomes (KEGG) database, no ^{18}O-labeling analytical methods were yet developed for phosphate-free metabolites and pathways. The advantage of such approach is the ability to calculate turnover rates of a large number of metabolites that will give us information not only about the dynamics of the entire metabolic system [2,8,25].

The Krebs cycle is the final stage of chemical processes that enable living cells to gain energy by oxidizing nutrients and plays an important role in all living organisms. The biochemical reactions in the Krebs cycle are catalyzed by eight different enzymes that are altered and can be used for monitoring of the different types of cancer [26,27]. Recent studies have demonstrated that multiple cycle enzymes are mutated or deregulated in various types of cancer, resulting in characteristic metabolic and epigenetic changes associated with disease progression [28]. Consequently, the ability to calculate turnover rates of the metabolites in the TCA cycle can be used to evaluate therapeutic efficacy of the treatment of different human diseases.

The aim of this study was to develop an ^{18}O stable isotope labeling method to monitor turnover rates of Krebs cycle intermediates in living cells using GC-MS. Labeling was achieved by incubating cells with ^{18}O-water containing media, and the percentage of ^{18}O incorporation into Krebs cycle metabolites was determined. The developed method was applied to trace changes in Krebs cycle dynamics in human colon adenocarcinoma cell lines (Caco-2) as compared to human fetal colon cell lines (FHC), which are commonly used as in vitro cell culture models in colorectal cancer research.

2. Materials and methods

2.1. Cell culture study

Cell culture of Caco-2 was suspended with 10% fetal bovine serum, 2 mM L-glutamine, 100 units/mL penicillin G, 100 μg/mL streptomycin, and 1% essential non-amino acid solution in Dulbecco's Modified Eagle Medium (DMEM). Cell culture of FHC was suspended with 10% fetal bovine serum, 5 μg/mL insulin transferrin selenium, 100 ng/mL hydrocortisone, 10 mM 4-(2-hydroxyethyl)-1-piperazine ethanesulfonic acid (HEPES), 100 units/mL penicillin G, 100 μg/mL streptomycin in Dulbecco's Modified Eagle Medium/Nutrient Mix F-12 (DMEM-F12) (1:1, v/v). All cultures were harvested at 37 °C containing 5% CO_2 in cell lines that reached 100% confluency.

2.2. ^{18}O labeling of cell lines

Petri dishes with cell lines that reached 100% confluency were taken out from the incubator and quickly washed with isotonic sodium chloride solution. Then 10 mL of cell medium containing 30% $H_2[^{18}O]$ (Rotem Industries Ltd., Israel) was added and incubated at 37 °C at three different times, which were 1, 2, and 5 min. After completing the labeling period, the cells were taken out from the incubator, and the labeling medium was removed, and cells washed rapidly with isotonic sodium chloride solution. Afterward, 1 mL of ice-cold methanol:water (9:1, v/v) was added, and the cells were quickly frozen in liquid nitrogen to quench cells' metabolism. Methanol:water mixture is a suitable solvent for extraction of all primary and secondary metabolites as it has good penetration to

the cell conten. This technique assures rapid quenching of metabolism and is used for ^{13}C-flux analysis and stable isotope labeling in cell culture [29]. The frozen cells were scraped off with cell scraper into Eppendorf tubes. The Petri dishes were washed by adding 1 mL of a mixture of ice-cold methanol:water (9:1, v/v), and the extracts were combined. After the extracts were centrifugated at 15,000 rpm at 4 °C for 10 min and the supernatant was transferred to a 2 mL Eppendorf tube and stored at −80 °C until analysis.

2.3. Derivatization

400 μL supernatant of each sample were transferred into an Eppendorf tube and completely dried in a vacuum concentrator at 4 °C to avoid metabolite degradation. 20 μL methoxyamine hydrochloride in pyridine was added over the dried sample in order to prevent the formation of multiple derivatives when enols are present during silylation and samples incubated 90 min at 30 °C. Then, samples derivatized using 80 μL of N-methyl- N-trimethylsilyl trifluoroacetamide (MSTFA) and 1% trimethylchlorosilane (TMCS) 30 min at 37 °C. Both of the reagents are creating silyl derivatives of the metabolites. But the TMCS, a catalyst, increases the silylation efficiency. Therefore MSTFA with 1% TMCS was used for derivatization.

2.4. GC-MS measurements

The derivatized samples were transferred into silanized GC-MS vials and analyzed using a Gas Chromatography-Mass Spectrometer (GC-MS QP2010 Ultra system, Shimadzu, Japan) with Agilent DB5-MS (30 m, 0.25 mm, 0.25 μm) column. The injection volume was set 1 μL in splitless mode. The oven temperature was held constant at 60 °C for 1 min and ramped at 10 °C/min to 200 °C then ramped at 30 °C/min to 320 °C and held for 6 min before cool-down. Electron ionization (EI) were performed at 70 eV. The delay time of carrier gas and MSD transfer line temperature were set 5.90 min and 290 °C, respectively. Data were acquired over the range of *m*/*z* of 50−650 in scan mode. Helium was carrier gas with 1 mL/min flow rate.

2.5. Data analysis and calculation of turnover rates

Each labeled oxygen in metabolites via $H_2[^{18}O]$ causes an increase in the mass of 2 m/z according to the number of oxygens interacting with the molecule. For example, ions (*m*/*z*) of citrate for each oxygen (^{16}O, $^{18}O_1$, $^{18}O_2$, ….. and $^{18}O_7$) were monitored at unlabeled ion (^{16}O) +2, +4, … …. and +14, respectively. The labeling percentages of metabolites via ^{18}O were calculated using the peak areas of each labeled isotopes. On the other hand, turnover rates of metabolites can be calculated by labeling percentage of metabolites. For this reason, the peak area of the metabolite at each amu (isotopologue distribution) was calculated after correction of the contribution of naturally occurring isotopes obtained from unlabeled samples. These values were used to calculate the total labeling percentage of ^{18}O by the following formula as described in Refs. [8,30].

$$\text{Total } ^{18}\text{O labeling } \% = \left(\sum_{i=1}^{n} i \; x \; ^{18}O_i \% \right) / n \; x \; H_2 \left[^{18}O \right] \%$$

n: Total labeled oxygen in molecule
i: Number of labeled oxygen with $H_2[^{18}O]$
The turnover rate is calculated using a total value of ^{18}O labeling.

$SA_t = 1\text{-}(2^{-N})$
SA_t: Specific activity (Total enreachment % at the end of the labeling period)
N: Number of turnover cycles

3. Results and discussion

Calculating turnover rates of energy pathways provides unique information in understanding the mechanism of disease in addition to the metabolic profile. ^{18}O percentage of phosphate metabolites can be detected via ^{31}P NMR and mass spectrophotometer. However, for Krebs cycle metabolites, incorporation of ^{18}O percentage cannot be detected with NMR, since ^{18}O cannot create a chemical shift on ^{1}H NMR and Krebs cycle metabolites do not contain phosphate. Therefore, mass spectrometry is the only method for this analysis. There are 2 amu changes of mass in mass spectra for each oxygen atom, and using these differences, the turnover rates and turnover times of the respective pathways can be calculated by determining the percentage of ^{18}O integration with Krebs cycle metabolites.

3.1. Mechanism of the labeling

^{18}O is a natural and stable isotope and can be used for the labeling of phosphate-containing and non-phosphate metabolites. When a tissue or cell is exposed to media containing water with a known percentage (20−30%) of ^{18}O, there is potential to label all metabolites in which the water is involved in enzymatic reactions. From this point of view, Krebs cycle metabolites can be labeled because of incorporation of $H_2[^{18}O]$, inorganic phosphate and acetyl coenzyme at 5 different positions in the cycle (Fig. 1A). All metabolites in the Krebs cycle are labeled with ^{18}O at the end of the first cycle (Fig. 1B). Krebs cycle is a continuous process. In the second and subsequent cycles, there is no change in the labeled oxygen positions of metabolites in the Krebs cycle (Fig. 1B and C). This indicates that the Krebs cycle metabolites can be determined in a stable manner, and the labeling percentages of each metabolite are associated with the number of turnovers.

3.2. Selection of mass fragments for labeling calculations

The selection of the appropriate fragment plays a critical role in performing accurate analyses. The selected *m*/*z* values must be covering the intact molecules, otherwise the incorporation percentage of ^{18}O into molecules may misleading. Therefore, for each Krebs cycle mediator, standards were prepared and run on the instrument to determine retention time and to obtain spectrum. The molecular ion fragment or closest fragment ion from spectra was selected for monitoring instead of the base peak fragment. The high energy used for ionization in GC-MS disintegrates compounds into small fragments. The product ions with biggest *m*/*z* value of each metabolite in spectrum was used for calculation of labeling percentages of ^{18}O and turnover rates. This allows us to correctly monitor all oxygen incorporation in the metabolite (Fig. 2). The retention index and selected *m*/*z* values of each Krebs cycle metabolite monitored as trimethylsilyl derivative was given in Table 1.

3.3. Optimization of chromatographic conditions

The effect of the analysis time was optimized especially for selectivity. Because each ^{18}O incorporation into a metabolite will cause 2 amu increase in metabolite spectrum (Fig. 3), this increase may lead an interference, if the metabolites are coeluted. Such as fumarate and succinate must be separated from each other. Because

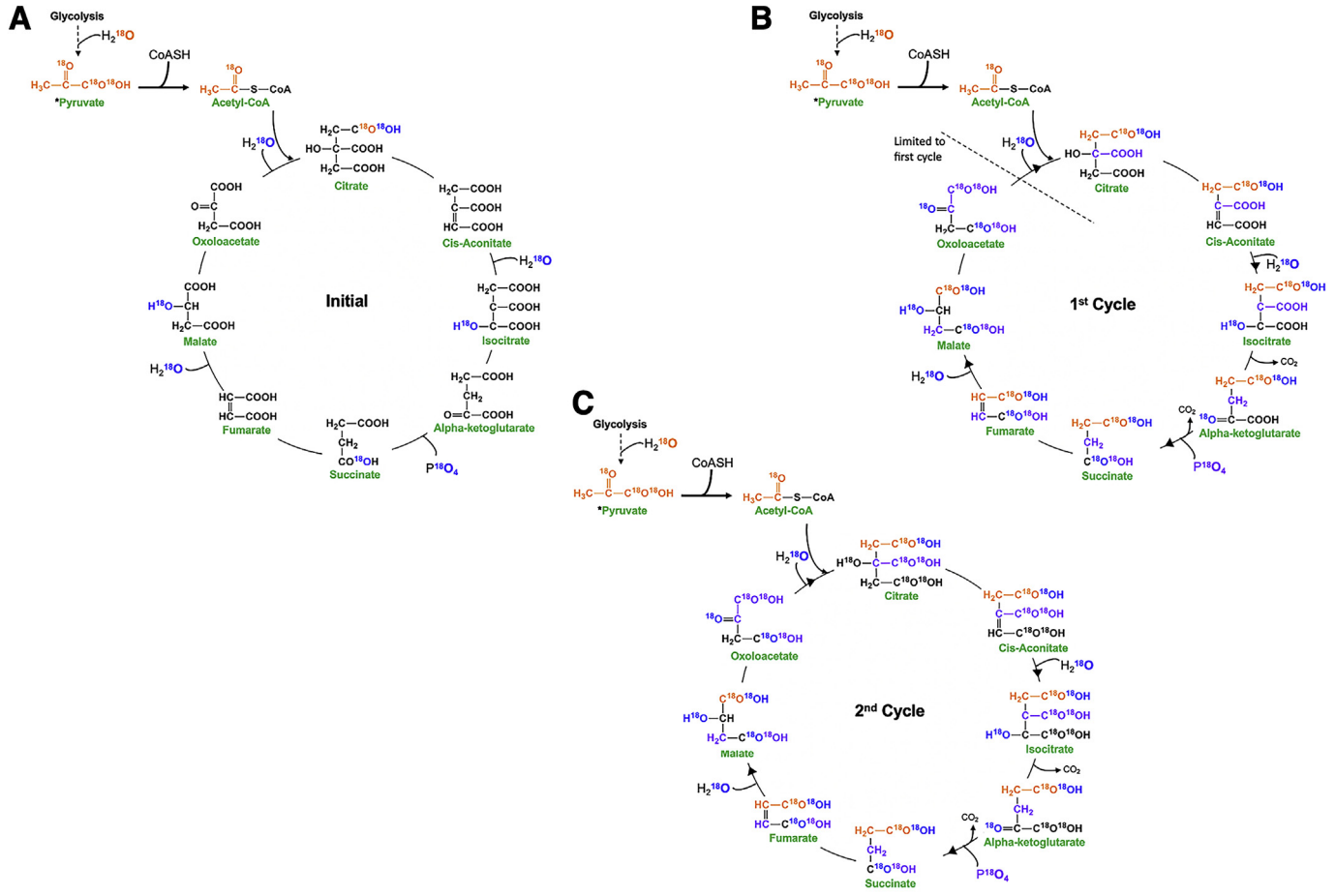

Fig. 1. Incorporation starting positions of ^{18}O in Krebs Cycle metabolites (A) labeling sites of Krebs cycle metabolites at the end of the first cycle (B) and second cycle (C) * The ^{18}O labeling of pyruvate were done through glycolysis.

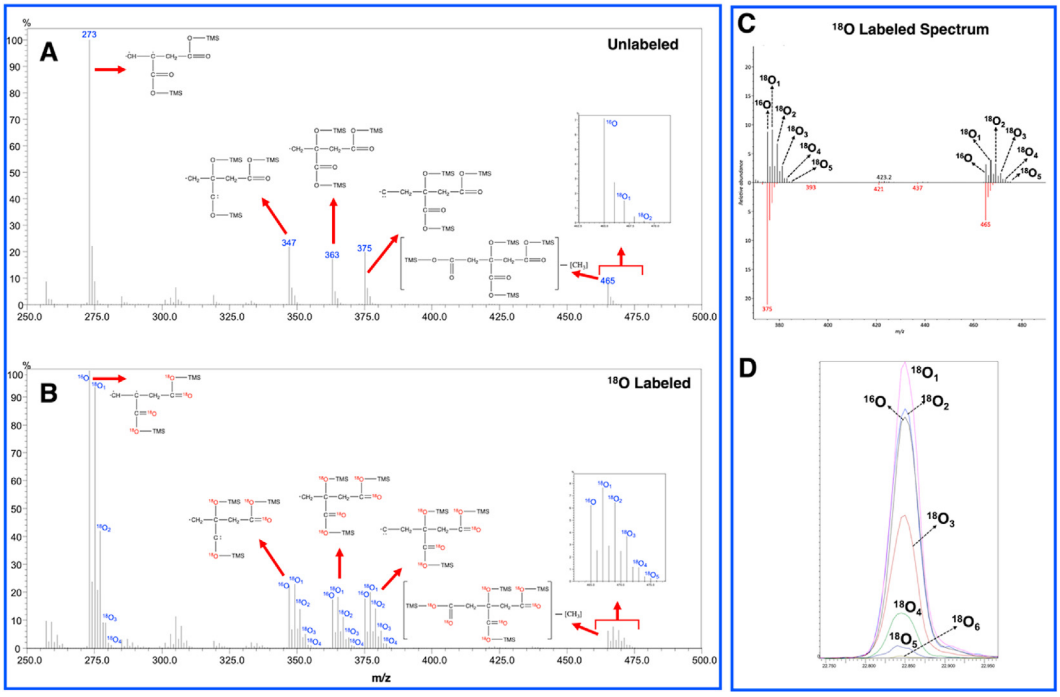

Fig. 2. Mass spectrum of citrate A) unlabeled, B) and C) labeled with 100% $H_2[^{18}O]$ for 24 h and D) peak of labeled citrate with 100% $H_2[^{18}O]$.

Table 1
Mass ions (*m/z*) of Krebs Cycle metabolites that correspond to ^{18}O-labeling ratio monitored as trimethylsilyl derivatives.

	Retention Index[a]	^{16}O	$^{18}O_1$	$^{18}O_2$	$^{18}O_3$	$^{18}O_4$	$^{18}O_5$	$^{18}O_6$	$^{18}O_7$
Alpha-ketoglutarate	1250	288	290	292	294	296	298		
Cis-aconititate	1423	375	377	379	381	383	385	387	
Fumarate	1025	245	247	249	251	253			
Iso-citrate	1498	465	467	469	471	473	475	477	479
Malate	1165	233	235	237	239	241	243		
Oxaloacetate	1139	290	292	294	296	298	300		
Citrate	1494	465	467	469	471	473	475	477	479
Succinate	990	247	249	251	253	255			

[a] Calculated using fatty acid methyl esters (FAME).

the unlabeled *m/z* value (247 m/z) of succinate is the same as the fumarate isotope *m/z* value (247 m/z) where an ^{18}O incooporated with fumarate (Fig. 3). In addition, other endogenous substances should not interfere with the targeted metabolites as a result of 2 m/z increase in mass. Therefore, it should be demonstrated that there is no interference at all working *m/z* values with unlabeled samples. For this purpose, unlabeled cell extract samples were analyzed using GC-MS, and spectrums were compared with pure standards. The matched scores were over 0.90 for all metabolites. Moreover, the number of coeluted peaks were evaluated after deconvolution of the peaks with Automated Mass Spectral Deconvolution and Identification System (AMDIS v. 2.71), and the number of the peak eluate at the retention times of the metabolites was one. These results indicate that the method had sufficient selectivity for isotope calculation.

3.4. Optimization of labeling time

1, 2, and 5 min of labeling FHC and Caco-2 cell lines with ^{18}O were separately prepared as described in the Materials section. For each labeling time, a 400 μL methanol extract was taken, evaporated to dryness, and derivatized. The labeling ratio of the metabolites increased with incubation time (Fig. 4). The labeling time must be ended before saturation. As seen in Fig. 5, the labeling ratio of the metabolites does not reach the saturation level since the labeling ratio was less than 30%. Any of this incubation time can be selected for the monitoring of the labeling ratio. In our case, we selected 5 min because of its highest labeling ratio. On the other hand, if the labeling ratio calculation includes phosphate metabolites, this time may be higher for monitoring of them. Based on the aim and cell type, the labeling ratio must be determined.

3.5. Application of ^{18}O-labeling of Krebs cycle metabolites to cancerous Caco-2 and control FHC cell lines

The Krebs cycle represents a metabolic pathway playing an essential role in tumor formation and progression [27,31]. The Krebs cycle occurs in the mitochondrial matrix, where multiple metabolic energy transduction pathways converge. Modification of the Krebs cycle is part of the rewiring of cancer cell energy metabolism to promote cancer cell proliferation [31,32]. Moreover, Krebs cycle metabolites are potent metabolic signaling molecules involved in epigenetic remodeling and post-translational protein modifications that affect the initiation and progression of carcinogenesis [27,33,34]. Colorectal cancer is one of the leading causes of cancer-related deaths, although significant advances have been made in its treatment in recent years [26]. Metabolic changes in cancer cells are numerous and these increase the formation of

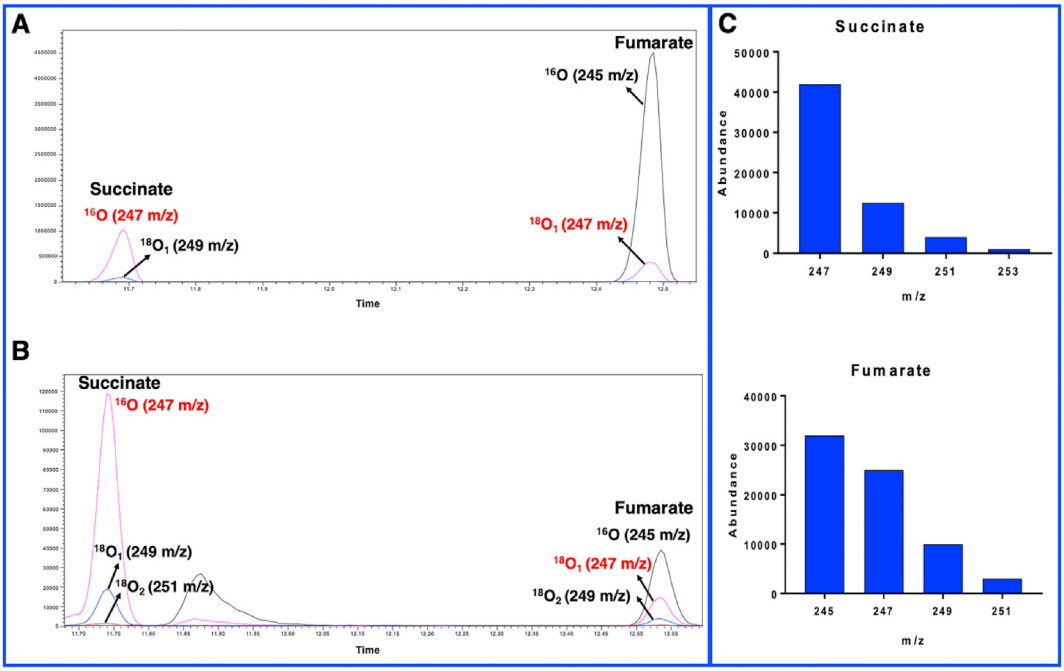

Fig. 3. Analysis of ^{18}O-incorporation into succinate and fumarate; extracted ion chromatograms of A) standards and B) labeled cell extracts with 30% $H_2[^{18}O]$ for 5 min.

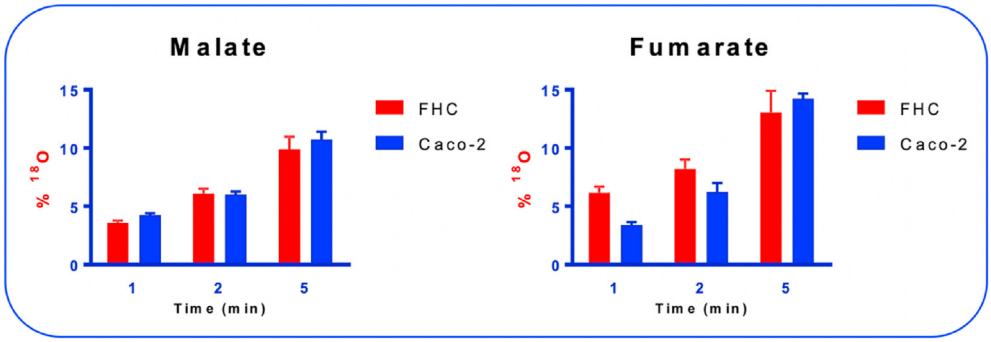

Fig. 4. The effect of the incubation time on labeling ratio of the metabolites. The effect of the labeling percentage of 1, 2 and 5 min incubation time with 30% $H_2[^{18}O]$ on FHC and Caco-2 cell lines.

biosynthetic intermediates needed for aerobic glycolysis, reduced oxidative phosphorylation, and cell growth and proliferation [27,31,32,35]. While healthy cells completely consume glucose at normal oxygen levels, cancer cells can partially break down glucose even at low oxygen levels. For this reason, normal cells cannot live in an oxygen-free environment, while cancer cells can grow and develop in an oxygen-limited climate [36,37]. Under conditions where pO_2 is normal, oxidative phosphorylation occurs, and the pyruvate enters the Krebs cycle. In order to better understand the cancer mechanism in eukaryotic cells, it is important to monitor the dynamic changes of metabolites in the Krebs cycle, which plays a major role in energy transduction.

Here, we used stable isotope ^{18}O-tracer to label Krebs cycle intermediates in intact Caco-2 cells as cancer model and FHC cells as controls. As presented in Fig. 6, cancerous Caco-2 cells had lower citrate ^{18}O-labeling, accordingly number of turnover cycle decreased from 0.371 ± 0.028 in FHC cells to 0.252 ± 0.011 in Caco-2 cells ($p = 0.014$). Labeling of cis-aconitate also was lower and turnover cycle decreased from 0.216 ± 0.034 in FHC cells to 0.114 ± 0.006 in Caco-2 cells ($p = 0.043$) (Table 2). Labeling with ^{18}O of isocitrate and alpha-ketoglutarate had higher variation, and no significant differences were detected ($p > 0.05$). Similarly, succinate labeling was unchanged too (Table 2). The fumarate ^{18}O-labeling and number of turnover cycle was decreased from 0.326 ± 0.016 in FHC cells to 0.229 ± 0.008 in Caco-2 cells ($p = 0.007$). Turnover cycle of malate was significantly reduced in Caco-2 cells as compared to control FHC cells at 0.176 ± 0.034 and 0.411 ± 0.016, respectively ($p = 0.002$). ^{18}O-labeling data indicates a pattern of lower Krebs cycle turnover in Caco-2 cells. Thus, compared to the control group (FHC), the Krebs cycle flux is reduced in Caco-2 that prefer glycolysis instead of the oxidative phosphorylation pathway. The ability of cancer cells to consume higher amounts of glucose at low oxygen levels is described in the literature as the "Warburg Effect" [36]. Otto Warburg observed that cancer cells prefer glycolysis and fermentation instead of oxidative

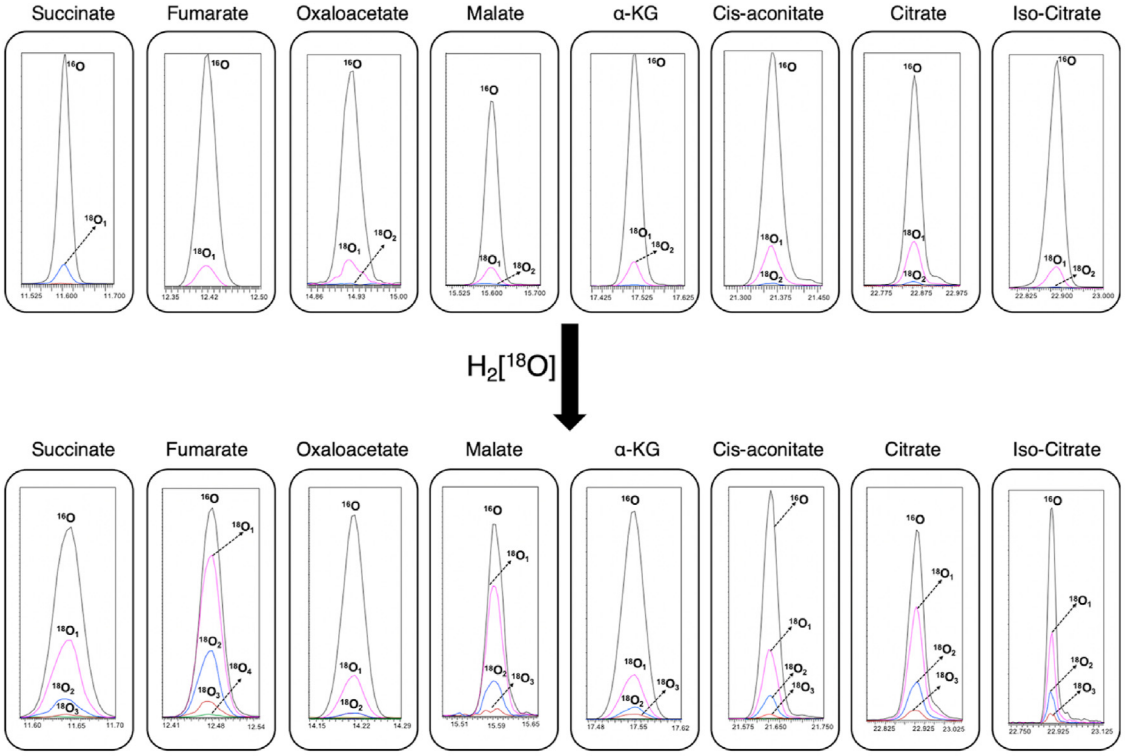

Fig. 5. The obtained chromatograms of the Krebs cycle metabolites before and after labeling with $H_2[^{18}O]$.

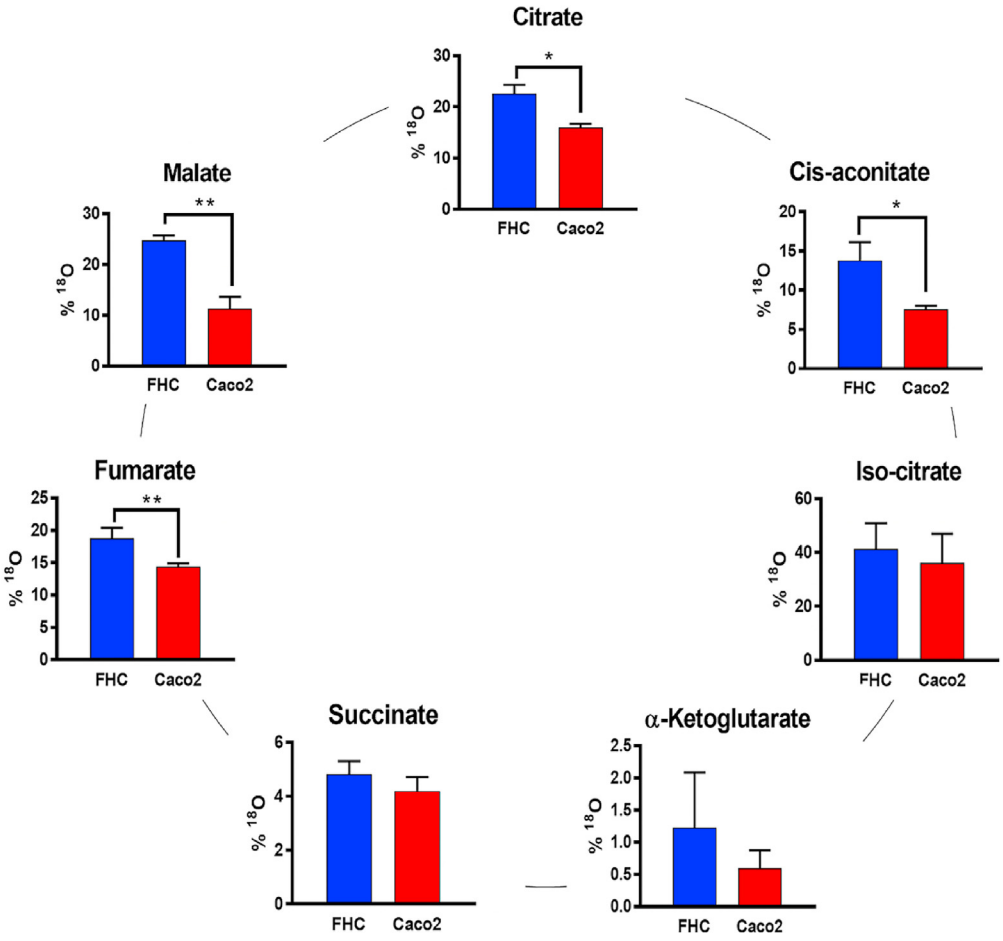

Fig. 6. The labeling rates of Krebs cycle metabolites in Caco-2 and FHC cell lines after incubation with 30% $H_2[^{18}O]$ for 5 min * - indicates statistical significance at $p < 0.05$. ** - indicates statistical significance at $p < 0.01$. Error bars represent standard error.

Table 2
Number of turnover cycles of Krebs cycle metabolites Caco-2 and FHC cell lines.

	Caco-2	FHC	p Value
Alpha-ketoglutarate	0.009 ± 0.004	0.018 ± 0.011	0.514
Cis-aconitate	0.114 ± 0.006	0.216 ± 0.034	0.043
Fumarate	0.229 ± 0.008	0.326 ± 0.016	0.007
Iso-citrate	0.712 ± 0.218	0.841 ± 0.238	0.741
Malate	0.176 ± 0.034	0.411 ± 0.016	0.002
Citrate	0.252 ± 0.011	0.371 ± 0.028	0.014
Succinate	0.062 ± 0.007	0.072 ± 0.006	0.394

phosphorylation. Cancer cells also prevent programmed cell death by disabling mitochondria and the reason for this is reduced oxidative capacity of mitochondria in cancer cells [36,37]. In addition to metabolic imaging approaches, basic mechanisms that define the heterogeneity of cancer cell metabolism will undoubtedly be better understood as the in vivo ^{18}O isotope monitoring methodology developed by us continues to be applied more broadly.

The ^{18}O-labeling pattern observed here is similar to that obtained using ^{13}C-labeling of Krebs cycle and other metabolites in cancer cells [27,31,35]. In renal cell carcinoma, ^{13}C-labeling of fumarate, malate, and citrate were depressed, as observed here with ^{18}O-labeling in Caco-2 cells [31]. However, ^{13}C-labeling revealed a lower turnover rate of succinate in renal carcinoma cells [31]. Thus, comparing different tracers can provide unique information concerning altered metabolic pathways in physiological and disease conditions [8,11]. Future experiments will compare simultaneous ^{18}O- and ^{13}C-labelings of metabolites to track oxygen and carbon exchange dynamics in cells and tissues.

4. Conclusions

Here, we developed a novel ^{18}O-labeling technique that can be used to measure the dynamics of Krebs cycle metabolites. Our results demonstrate that the $H_2[^{18}O]$ based as stable isotope carrier ^{18}O-labeling technique can be used not only for monitoring phosphoryl turnover, as traditionally used, but also for tracking oxygen exchange kinetics in Krebs cycle mediators. Optimal ^{18}O-labeling conditions and the highest m/z value of each metabolite fragment was determined for use in calculation of labeling percentages of ^{18}O and turnover cycles. The developed technique was applied to measure changes in Krebs cycle dynamics in cancerous Caco-2 cells as compared to the control FHC cells. The underlying mechanisms that define the heterogeneity of cancer cell metabolism will undoubtedly be better understood with the implementation of the in vivo ^{18}O isotope monitoring methodology developed by us. The choice of isotope labeling technique usually depends on the experimental design, sample type, and specific metabolic pathway. Moreover, the incubation time is also important. The ^{18}O-labeling can be completed within minutes as compared to the other techniques (^{32}P, ^{13}C, ^{15}N), which require much longer incubation times.

This permits ease of application and repetition of experiments at the desired level. Thus, ^{18}O-labeling of Krebs cycle metabolites expands the arsenal of techniques for monitoring dynamics of cellular metabolism. In the future, the ^{18}O-labeling technique can be applied to numerous other metabolic pathways where oxygen exchange with water takes place. In this way, dynamic metabolomic profiling of different systems can be compared via turnover rates of metabolites, and obtained detailed and unique information about the mechanism of the diseases, diagnostic and treatment potential can be obtained.

CRediT authorship contribution statement

Cemil Can Eylem: Conceptualization, Methodology, Formal analysis, Writing – original draft, Visualization. **İpek Baysal:** Methodology. **Acelya Erikci:** Methodology. **Samiye Yabanoglu-Ciftci:** Conceptualization, Methodology. **Song Zhang:** Conceptualization, Methodology, Writing - review & editing. **Sedef Kır:** Conceptualization, Methodology, Writing - review & editing. **Andre Terzic:** Conceptualization, Writing - review & editing. **Petras Dzeja:** Conceptualization, Methodology, Writing - review & editing. **Emirhan Nemutlu:** Conceptualization, Supervision, Methodology, Funding acquisition, Visualization, Writing - review & editing.

Declaration of competing interest

The authors declare that they have no known competing financial interests or personal relationships that could have appeared to influence the work reported in this paper.

Acknowledgment

This project (ID: 116Z292) was funded by The Scientific and Technological Research Council of Turkey (TÜBİTAK).

References

[1] W.B. Dunn, et al., Procedures for large-scale metabolic profiling of serum and plasma using gas chromatography and liquid chromatography coupled to mass spectrometry, Nat. Protoc. 6 (7) (2011) 1060–1083.
[2] E. Nemutlu, et al., 18O-assisted dynamic metabolomics for individualized diagnostics and treatment of human diseases, Croat. Med. J. 53 (6) (2012) 529–534.
[3] A. Cornish-Bowden, M.L. Cardenas, From genome to cellular phenotype - a role for metabolic flux analysis? Nat. Biotechnol. 18 (3) (2000) 267–268.
[4] N.J. Kruger, R.G. Ratcliffe, Insights into plant metabolic networks from steady-state metabolic flux analysis, Biochimie 91 (6) (2009) 697–702.
[5] W. Weckwerth, Metabolomics: Methods and Protocols, Humana Pr Inc, 2007.
[6] P.P. Dzeja, A. Terzic, B. Wieringa, Phosphotransfer dynamics in skeletal muscle from creatine kinase gene-deleted mice, Mol. Cell. Biochem. 256 (1–2) (2004) 13–27.
[7] E. Nemutlu, et al., Decline of phosphotransfer and substrate supply metabolic circuits hinders ATP cycling in aging myocardium, PloS One 10 (9) (2015), e0136556.
[8] E. Nemutlu, et al., Dynamic phosphometabolomic profiling of human tissues and transgenic models by 18O-assisted (3)(1)P NMR and mass spectrometry, Physiol. Genom. 44 (7) (2012) 386–402.
[9] M.R. Antoniewicz, J.K. Kelleher, G. Stephanopoulos, Elementary metabolite units (EMU): a novel framework for modeling isotopic distributions, Metab. Eng. 9 (1) (2007) 68–86.
[10] R. Nilsson, M. Jain, Simultaneous tracing of carbon and nitrogen isotopes in human cells, Mol. Biosyst. 12 (6) (2016) 1929–1937.
[11] D.M. Freund, A.D. Hegeman, Recent advances in stable isotope-enabled mass spectrometry-based plant metabolomics, Curr. Opin. Biotechnol. 43 (2017) 41–48.
[12] Z. Tang, M.V. Martin, F.P. Guengerich, Elucidation of functions of human cytochrome P450 enzymes: identification of endogenous substrates in tissue extracts using metabolomic and isotopic labeling approaches, Anal. Chem. 81 (8) (2009) 3071–3078.
[13] J. Kappelmann, et al., Comprehensive and accurate tracking of carbon origin of LC-tandem mass spectrometry collisional fragments for C-13-MFA, Anal. Bioanal. Chem. 409 (9) (2017) 2309–2326.
[14] J. Kappelmann, et al., Separation of C-13- and N-15-Isotopologues of amino acids with a primary amine without mass resolution by means of O-phthalaldehyde derivatization and collision induced dissociation, Anal. Chem. 91 (21) (2019) 13407–13417.
[15] S.M. Dawis, et al., *Adenosine triphosphate utilization rates and metabolic pool sizes in intact cells measured by transfer of ^{18}O from water*, Biophys. J. 55 (1) (1989) 79–99.
[16] P.P. Dzeja, R.J. Zeleznikar, N.D. Goldberg, Suppression of creatine kinase-catalyzed phosphotransfer results in increased phosphoryl transfer by adenylate kinase in intact skeletal muscle, J. Biol. Chem. 271 (22) (1996) 12847–12851.
[17] N. Juranic, et al., *^{31}P NMR correlation maps of ^{18}O/^{16}O chemical shift isotopic effects for phosphometabolite labeling studies*, J. Biomol. NMR 50 (3) (2011) 237–245.
[18] D. Pucar, et al., *Cellular energetics in the preconditioned state: protective role for phosphotransfer reactions captured by ^{18}O-assisted ^{31}P NMR*, J. Biol. Chem. 276 (48) (2001) 44812–44819.
[19] M.R. Antoniewicz, A guide to (13)C metabolic flux analysis for the cancer biologist, Exp. Mol. Med. 50 (4) (2018) 19.
[20] N. Juranic, et al., 31)P NMR correlation maps of (18)O/(16)O chemical shift isotopic effects for phosphometabolite labeling studies, J. Biomol. NMR 50 (3) (2011) 237–245.
[21] E. Nemutlu, et al., Electron spray ionization mass spectrometry and 2D 31P NMR for monitoring 18O/16O isotope exchange and turnover rates of metabolic oligophosphates, Anal. Bioanal. Chem. 403 (3) (2012) 697–706.
[22] P.P. Dzeja, A. Terzic, Phosphotransfer networks and cellular energetics, J. Exp. Biol. 206 (12) (2003) 2039–2047.
[23] E. Janssen, et al., Adenylate kinase 1 gene deletion disrupts muscle energetic economy despite metabolic rearrangement, EMBO J. 19 (23) (2000) 6371–6381.
[24] E. Janssen, et al., Impaired intracellular energetic communication in muscles from creatine kinase and adenylate kinase (M-CK/AK1) double knock-out mice, J. Biol. Chem. 278 (33) (2003) 30441–30449.
[25] P.P. Dzeja, et al., Rearrangement of energetic and substrate utilization networks compensate for chronic myocardial creatine kinase deficiency, Journal of Physiology-London 589 (21) (2011) 5193–5211.
[26] N.A.A. Hashim, et al., Global serum metabolomics profiling of colorectal cancer, Mol Clin Oncol 11 (1) (2019) 3–14.
[27] L.C. Tavares, et al., Metabolic evaluations of cancer metabolism by NMR-based stable isotope tracer methodologies, Eur. J. Clin. Invest. 45 (Suppl 1) (2015) 37–43.
[28] K. Sajnani, et al., Genetic alterations in Krebs cycle and its impact on cancer pathogenesis, Biochimie 135 (2017) 164–172.
[29] S.C. Sapcariu, et al., Simultaneous extraction of proteins and metabolites from cells in culture, Methods 1 (2014) 74–80.
[30] P.P. Dzeja, et al., Adenylate kinase-catalyzed phosphotransfer in the myocardium : increased contribution in heart failure, Circ. Res. 84 (10) (1999) 1137–1143.
[31] K.D. Courtney, et al., Isotope tracing of human clear cell renal cell carcinomas demonstrates suppressed glucose oxidation in vivo, Cell Metabol. 28 (5) (2018) 793–800 e2.
[32] A. Klepinin, et al., Adenylate kinase and metabolic signaling in cancer cells, Front Oncol 10 (2020) 660.
[33] C. Jang, L. Chen, J.D. Rabinowitz, Metabolomics and isotope tracing, Cell 173 (4) (2018) 822–837.
[34] C.J. Lio, S.C. Huang, Circles of Life: Linking Metabolic and Epigenetic Cycles to Immunity. Immunology, 2020.
[35] J. Zhang, et al., 13C isotope-assisted methods for quantifying glutamine metabolism in cancer cells, Methods Enzymol. 542 (2014) 369–389.
[36] O. Warburg, On respiratory impairment in cancer cells, Science 124 (3215) (1956) 269–270.
[37] Y. Zhao, E.B. Butler, M. Tan, Targeting cellular metabolism to improve cancer therapeutics, Cell Death Dis. 4 (2013) e532.